ACS APPLIED MATERIALS & INTERFACES

Research Article

www.acsami.org

Novel D-π-A Organic Dyes with Thieno[3,2-*b*]thiophene-3,4-ethylenedioxythiophene Unit as a π-Bridge for Highly Efficient Dye-Sensitized Solar Cells with Long-Term Stability

Min-Woo Lee,[†,‡] Jae-Yup Kim,[†] Duck-Hyung Lee,*[,‡] and Min Jae Ko*[,†,§]

[†]Photo-Electronic Hybrids Research Center, Korea Institute of Science and Technology, Seoul, 136-791, Republic of Korea

[‡]Department of Chemistry, Sogang University, Seoul, 121-742, Republic of Korea

[§]Green School, Korea University, 145, Anam-ro, Seongbuk-gu, Seoul, 136-701, Republic of Korea

Supporting Information

ABSTRACT: This paper reports on new D-π-A organic dyes for application in dye-sensitized solar cells (DSSCs), which were developed by incorporating thieno[3,2-*b*]thiophene-thiophene (**M9**) and thieno[3,2-*b*]thiophene-EDOT (**M10**) as π-bridges. These dyes exhibited relatively small highest occupied molecular orbital (HOMO)−lowest unoccupied molecular orbital (LUMO) energy gaps in spite of the short π-conjugation lengths, resulting in broad spectral responses. As photosensitizers in DSSCs, **M10** showed a broader spectral response than **M9**, leading to a greater short-circuit photocurrent (J_{sc}). In addition, **M10** exhibited higher open-circuit voltage (V_{oc}) compared to **M9**, because of the greater electron lifetime of the photoanode. The impedance analysis revealed that the greater electron lifetime of the photoanode with **M10** was attributed to the lower electron recombination rate caused by the blocking effect of the bulky EDOT unit. As a result, **M10** showed much higher conversion efficiency (η = 7.00%) than **M9** (η = 5.67%) under one sun condition (AM 1.5 G, 100 mW/cm^2). This conversion efficiency was comparable to that of the conventional Ru-based dye **N719** (η = 7.24%) under the same condition. In addition, **M10** exhibited a remarkable long-term stability, i.e., 95% of the initial conversion efficiency was maintained after light soaking for 45 days (1080 h).

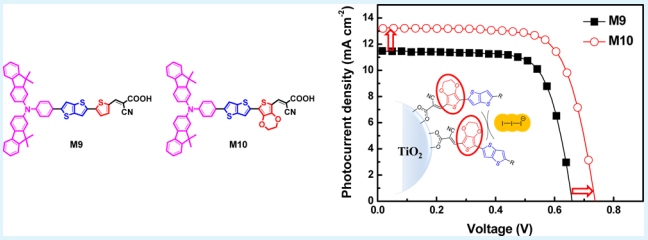

KEYWORDS: *donor−acceptor dyes, dye-sensitized solar cells, EDOT unit, spectral response, impedance spectroscopy*

INTRODUCTION

Over the last few decades, dye-sensitized solar cells (DSSCs) have been extensively investigated because they can be used as an alternative to conventional p−n junction silicon solar cells.[1] In DSSCs, the photosensitizer dye is the main component responsible for determining the light harvesting performance and the power conversion efficiency. Ruthenium complexes are typically used as sensitizers in high-efficiency DSSCs that exhibit conversion efficiency of more than 11%.[2,3] However, the widespread application of Ru is limited owing to its scarcity, high cost, and problems with isomerization during its purification.[4] To overcome the drawbacks of Ru-based dyes, metal-free organic dyes have been developed as alternative photosensitizers because they exhibit advantages such as low material cost, high molar extinction coefficients, and ease of purification.[5−9] However, the practical application of organic dyes is also limited, owing to drawbacks such as narrow absorption windows and unfavorable photovoltaic properties. To expand the light-absorption range of conventional organic dyes with a donor-π bridge-acceptor (D-π-A) configuration, methine (−CH═CH−) or aromatic units have been introduced to extend the π-conjugation.[10] However, the introduction of methine results in decreased stability because of an increase in the *cis-trans* photoisomerization of the C═C bonds.[11] In addition, the introduction of multiring (3−5) aromatic units to achieve a low highest occupied molecular orbital (HOMO)−lowest unoccupied molecular orbital (LUMO) energy gap generally leads to more complex synthetic routes that are not suitable for widespread applications.[12]

Besides, in order to enhance the open-circuit voltage (V_{oc}), linear alkyl chains were generally introduced into the dye framework, which suppress the approach of I_3^- ions in the electrolyte to the TiO_2 surface[13] However, this approach can increase the dihedral angle in the dye framework, resulting in the reduced overall π-conjugation and increased HOMO−LUMO energy gap.[14]

In this work, we developed new D-π-A organic dyes by incorporating thieno[3,2-*b*]thiophene-thiophene (**M9**) and thieno[3,2-*b*]thiophene-3,4-ethylenedioxythiophene (**M10**) as π-bridges (Chart 1), which provide superior photovoltaic performance as well as long-term stability. Through density functional theory (DFT) calculations, we estimated these dyes to have relatively small HOMO−LUMO energy gaps in spite of the short π-conjugation lengths, which is suitable for a wide

Received: December 11, 2013
Accepted: February 21, 2014
Published: February 21, 2014

   dx.doi.org/10.1021/am405686z | *ACS Appl. Mater. Interfaces* 2014, 6, 4102−4108

Chart 1. Molecular Structures of M9 and M10

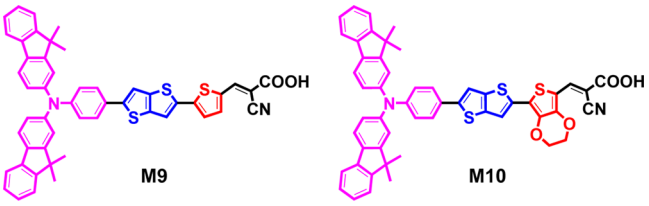

spectral response. In practice, **M10** exhibited a higher conversion efficiency (η = 7.00%) than that of a conventional Ru-based dye **N719** (η = 7.24%) under the same experimental conditions. It also exhibited a remarkable long-term stability under light-soaking conditions.

EXPERIMENTAL SECTION

Synthesis of *N*-(9,9-Dimethyl-9*H*-fluoren-2-yl)-9,9-dimethyl-*N*-(4-(thieno[3,2-*b*]thiophene-2-yl)phenyl)-9*H*-fluoren-2-amine (2). A mixture of **1** (3.06 g, 5.50 mmol), thieno[3,2-*b*]thiophene-2-ylboronic acid (1.24 g, 5.50 mmol), $Pd(PPh_3)_2Cl_2$ (386 mg, 0.55 mmol), and K_2CO_3 (7.6 g) in tetrahydrofuran (THF, 420 mL) and H_2O (100 mL) was stirred at 80 °C for 8 h. After cooling to room temperature, the reaction mixture was filtered through Celite; then, the filtrate was poured into water and extracted with EtOAc. The combined organic phases were washed with brine, dried with Na_2SO_4, and then concentrated *in vacuo*. The crude residue was purified by column chromatography to give adduct **2** (2.14 g, 63%) as yellow solid. ^{1}H NMR (300 MHz, $CDCl_3$, δ): 7.67−7.60 (m, 4H), 7.54−7.51 (m, 2H), 7.42−7.39 (m, 4H), 7.26 (brs, 4H), 7.22−7.18 (d, 2H), 7.14 (brs, 2H), 1.42 (s, 12H). ^{13}C NMR (300 MHz, $CDCl_3$, δ): 156.1, 154.4, 148.1, 147.9, 147.9, 139.8, 139.8, 135.5, 135.4, 134.8, 134.7, 134.6, 134.5, 133.2, 133.1, 133.0, 129.6, 129.5, 129.4, 128.0, 127.6, 127.5, 126.3, 126.2, 124.1, 123.8, 123.5, 121.7, 121.6, 120.5, 120.4, 119.6, 115.8, 115.7, 78.2, 78.0, 77.8, 47.8, 47.7, 28.0, 27.9, 27.8. LRMS (ESI, *m*/*z*): $[M]^+$ calcd for $C_{42}H_{33}NS_2$, 615; found, 615.38.

Synthesis of *N*-(9,9-Dimethyl-9*H*-fluoren-2-yl)-9,9-dimethyl-*N*-(4-(5-(4,4,5,5-tetramethyl-1,3,2-dioxaborolan-2-yl)thieno-[3,2-*b*]thiophene-2-yl)phenyl)-9*H*-fluoren-2-amine (3). *n*-BuLi (2.25 M, 0.32 mL) was added dropwise to a solution of **2** (300 mg, 0.49 mmol) in THF (3 mL) at −25 °C. After stirring at 0 °C for 2 h, 2-isopropoxy-4,4,5,5-tetramethyl-1,3,2-dioxaborolane (0.15 mL, 0.74 mmol) was added at −78 °C. The reaction mixture was stirred at room temperature overnight. The organic layer was separated and the aqueous layer extracted with CH_2Cl_2. The combined organic phases were washed with brine, dried with Na_2SO_4, and concentrated *in vacuo*. The crude residue was purified by column chromatography to give adduct **3** (221 mg, 61%). ^{1}H NMR (300 MHz, $CDCl_3$, δ): 7.66−7.64 (dd, 2H), 7.62 (s, 1H), 7.60 (s, 1H), 7.53−7.51 (dd, 2H), 7.42 (s, 1H), 7.40 (s, 1H), 7.38 (s, 2H), 7.40−7.32 (m, 2H), 7.30−7.28 (dd, 2H), 7.27−7.26 (d, 1H), 7.25−7.24 (m, 1H), 7.23 (s, 1H), 7.20−7.18 (dd, 2H), 7.13−7.11 (dd, 2H), 1.42 (s, 12H), 1.26 (s,12H). ^{13}C NMR (300 MHz, $CDCl_3$, δ): 155.3, 153.7, 147.9, 147.1, 146.5, 140.4, 139.1, 138.0, 134.6, 128.9, 127.2, 126.8, 126.7, 126.5, 123.8, 123.5, 122.7, 120.8, 119.8, 119.6, 119.0, 114.5, 75.2, 68.1, 47.0, 27.2, 25.8, 25.0, 24.7. LRMS (ESI, *m*/*z*): $[M]^+$ calcd for $C_{48}H_{44}BNO_2S_2$, 741; found, 741.32.

Synthesis of 5-(5-(4-(Bis(9,9-dimethyl-9*H*-fluoren-2-yl)-amino)phenyl)thieno[3,2-*b*]thiophene-2-yl)thiophene-2-carbaldehyde (4). A mixture of **3** (200 mg, 0.27 mmol), 5-bromo-2-thiophenecarboxaldehyde (62 mg, 0.32 mmol) and $Pd(PPh_3)_2Cl_2$ (17 mg, 0.024 mmol), K_2CO_3 (373.2 mg) in THF (20 mL), H_2O (5.1 mL) was stirred at 80 °C overnight. After cooling to room temperature, the reaction mixture was filtered through Celite, and the filtrate was poured into water and extracted with EtOAc. The combined organic phases were washed with brine, dried with Na_2SO_4, and concentrated *in vacuo*. The crude residue was purified by column chromatography to give adduct **4** (100 mg, 51%). ^{1}H NMR (300 MHz, $CDCl_3$, δ): 9.89 (s, 1H), 7.76−7.75 (s, 1H), 7.67 (brs, 3H), 7.62−7.56 (m, 3H), 7.51−7.49 (d, 2H), 7.45−7.44 (d, 2H), 7.39−7.37 (d, 2H), 7.36−7.28 (m, 2H), 7.26 (s, 2H), 7.22−7.20 (d, 2H), 7.12−7.07 (m, 3H), 1.26 (s, 12H). ^{13}C NMR (300 MHz, $CDCl_3$, δ): 182.6, 155.5, 154.4, 146.9, 137.4, 132.3, 132.2, 130.1, 127.2, 127.1, 126.9, 126.7, 126.6, 125.9, 125.8, 125.6, 125.5, 123.6, 123.5, 123.4, 123.3, 122.9, 122.8, 122.4, 121.0, 120.9, 120.8, 120.7, 120.6, 120.4, 119.9, 119.4, 118.8, 117.9, 47.0, 29.2, 26.9, 26.8, 26.7. LRMS (ESI, *m*/*z*): $[M]^+$ calcd for $C_{47}H_{35}NOS_2$, 725; found, 725.42.

Synthesis of 7-(5-(4-(Bis(9,9-dimethyl-9*H*-fluoren-2-yl)-amino)phenyl)thieno[3,2-*b*]thiophene-2-yl)-2,3-dihydrothieno[3,4-*b*][1,4]dioxine-5-carbaldehyde (5). A mixture of **3** (200 mg, 0.27 mmol), 7-bromo-2,3-dihydrothieno[3,4-*b*][1,4]-dioxine-5-carbaldehyde (79.7 mg, 0.32 mmol), $Pd(PPh_3)_2Cl_2$ (17 mg, 0.024 mmol), and K_2CO_3 (373.2 mg) in THF (20 mL) and H_2O (5.1 mL) was stirred at 80 °C overnight. After cooling to room temperature, the reaction mixture was filtered through Celite, and the filtrate was poured into water and extracted with EtOAc. The combined organic phases were washed with brine, dried with Na_2SO_4, and concentrated *in vacuo* to yield 250 mg of **5** crude, which was directly in the next step.

Synthesis of M9. A solution of **4** (100 mg, 0.14 mmol) in chloroform (2 mL) and acetonitrile (1 mL) was added to cyanoacetic acid (23.8 mg, 0.28 mmol) and piperidiine (3.5 mg, 0.042 mmol). The mixture was refluxed for overnight, extracted with $CHCl_3$, and dried over $MgSO_4$. The combined organic phases were washed with brine, dried with Na_2SO_4, and concentrated *in vacuo*. The crude residue was purified by column chromatography to give adduct **M9** (68 mg, 61%). ^{1}H NMR (300 MHz, DMSO, δ): 8.25 (s, 2H), 7.94 (s, 2H), 7.88−7.65 (m, 5H), 7.49−7.43 (m, 5H), 7.26 (s, 4H), 7.03−6.99 (m, 5H), 1.35 (s, 12H). ^{13}C NMR (300 MHz, DMSO, δ): 164.3, 164.2, 155.5, 155.0, 154.3, 153.3, 148.8, 146.8, 146.3, 140.2, 138.2, 136.0, 134.3, 132.3, 131.4, 125.5, 125.3, 124.3, 123.3, 122.7, 121.6, 121.3, 120.1, 119.4, 118.9, 118.7, 114.3, 109.6, 46.3, 26.3. LRMS (ESI, *m*/*z*): $[M]^+$ calcd for $C_{50}H_{36}N_2O_2S_3$, 793; found, 792.50.

Synthesis of M10. A solution of **5** crude (250 mg, 0.32 mmol) in chloroform (2 mL) and acetonitrile (1 mL) was added to cyanoacetic acid (54.4 mg, 0.64 mmol) and piperidiine (8.2 mg, 0.096 mmol). The mixture was refluxed for overnight, extracted with $CHCl_3$, and dried over $MgSO_4$. The combined organic phases were washed with brine, dried with Na_2SO_4, and concentrated *in vacuo*. The crude residue was purified by column chromatography to give adduct **M10** (41 mg) as a plum solid. ^{1}H NMR (300 MHz, DMSO, δ): 8.01 (s, 2H), 8.00 (s, 1H), 7.79−7.69 (m, 5H), 7.61−7.60 (d, 2H), 7.49−7.48 (d, 2H), 7.30−7.26 (m, 5H), 7.11−7.06 (dd, 2H), 7.00 (s, 2H), 4.24 (s, 4H), 1.34 (s, 12H). ^{13}C NMR (300 MHz, DMSO, δ): 164.5, 163.9, 155.0, 153.3, 146.1, 145.3, 144.6, 141.3, 140.4, 138.2, 138.0, 136.3, 135.2, 134.3, 134.0, 129.4, 127.1, 126.9, 123.8, 122.7, 121.9, 121.3, 119.7, 119.4, 119.3, 111.9, 111.8, 106.3, 98.1, 93.7, 64.9, 64.3, 46.7, 26.4. LRMS (ESI, *m*/*z*): $[M]^+$ calcd for $C_{52}H_{38}N_2O_4S_3$, 851; found, 850.42.

Fabrication of DSSCs. The fluorine-doped tin oxide (FTO) glass (Pilkington, 2.3 mm thick, TEC-8, 8 Ω/sq) substrates were washed with ethanol using an ultrasonic bath for 10 min and then treated with UV/O_3 plasma for 20 min to remove organic residues. A thin TiO_2 compact layer was deposited on the FTO glass by spin-coating of 0.15 M Ti(IV) bis(ethyl acetoacetato)-diisopropoxide (Aldrich) solution in 1-butanol, followed by heating at 500 °C for 10 min. A paste was prepared using nanocrystalline TiO_2 particles with a 20 nm diameter that was synthesized by a hydrothermal method.[15] After the TiO_2 paste was deposited to the TiO_2 compact layer/FTO glass substrate by the Dr. Blading method, the TiO_2-paste coated FTO glass was annealed at 500 °C for 30 min. Then, a scattering paste containing 400 nm-sized TiO_2 particles (CCIC) was deposited on the annealed TiO_2 films, followed by an annealing at 500 °C for 30 min. The resulting film was composed of a 10 μm-thick nanoparticle layer with a 5 μm-thick scattering layer. The annealed TiO_2 film was immersed overnight in chloroform solution including 0.5 mM of the dye. A counter electrode was prepared by casting a drop of 0.7 mM H_2PtCl_6 in 2-propanol solution onto a FTO glass substrate, followed by annealing at 400 °C for 20 min in air. The counter electrode and the dye-adsorbed TiO_2 electrode were assembled using 60 μm-thick Surlyn (Dupont 1702). Measured under irradiation of AM 1.5 G simulated solar light

dx.doi.org/10.1021/am405686z | ACS Appl. Mater. Interfaces 2014, 6, 4102−4108

Scheme 1. Synthetic Route of M9 and M10

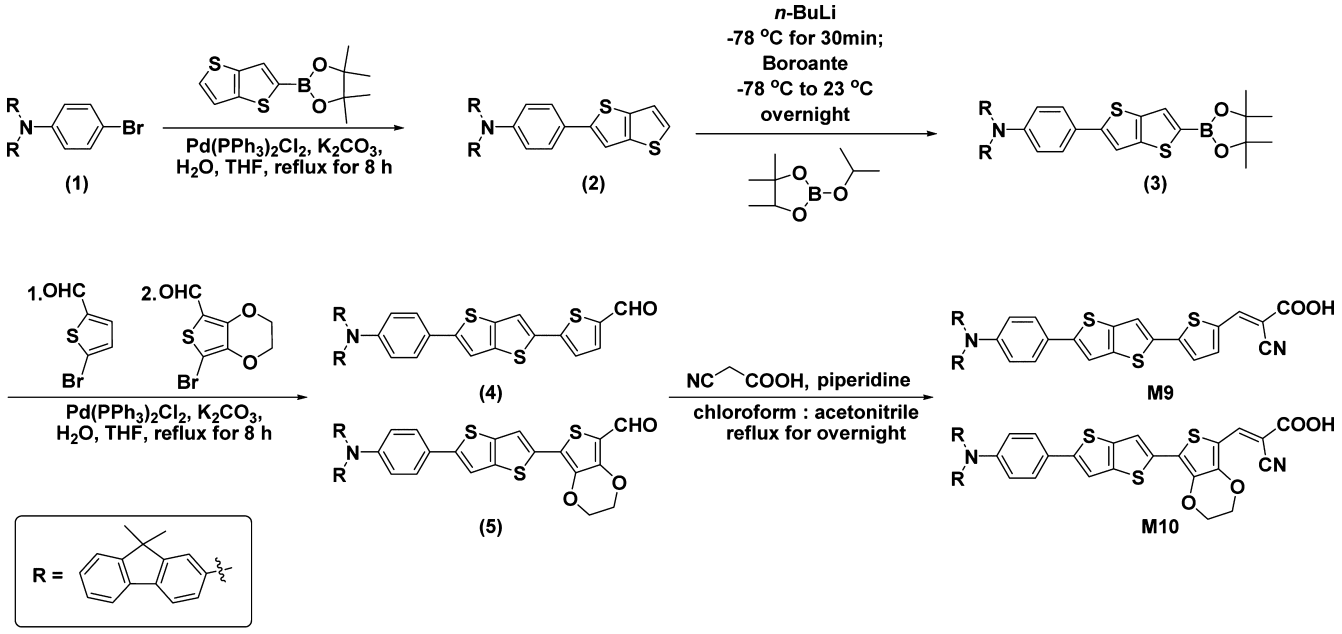

(100 mW cm^{-2}) at 23 °C, the active area was 0.450 cm^2, which was measured by an image analysis program equipped with a CCD camera (moticam 1000).

Characterizations. UV−vis spectra of the dyes dissolved in chloroform were obtained by using Agilent 8453 with a quarts cell. Cyclic voltammetry (CV) measurements were obtained using CH instrument (CHI 600C) with a three-electrode cell. The saturated calomel electrode (SCE) was used as a reference electrode, and a Pt disk and wire were used as working and counter electrode, respectively. The electrolyte was prepared by dissolving 1 mM of dye or ferrocene (Fc) and 0.1 M tetramethylammonium tetrafluoroborate (TMATFB) in THF. The scan rate was 0.1 V/s. The redox potentials of dyes were determined versus Fc and, then, converted to the values versus a normal hydrogen electrode (NHE). The thickness of the TiO_2 film was measured by Alpha-Step IQ surface profiler (KLA Tencor). To compare the dye loading, the adsorbed dye molecules on the 10 μm-thick nanocrystalline TiO_2 films were desorbed in 1 M NaOH aqueous solution and then examined by UV−vis spectroscopy. The dye loading per geometric area (1 cm^2) was calculated by comparing the absorption data for the dye solutions of known concentrations. Photocurrent−voltage (J−V) measurements were performed using a Keithly model 2400 source measure unit. The solar simulator (yamasita) equipped with a 1000 W Wenon lamp was used as a light source. The light intensity was adjusted with an NREL-calibrated Si solar cell with KG-5 filter. A black aperture mask was attached on the cells during the measurements.[16] Incident photon-to-current conversion efficiency (IPCE) was measured as a function of wavelength ranging from 300 to 800 nm using a specially designed IPCE system for DSSCs (PV measurements, Inc.). A 75 W xenon lamp was used as a light source for generating monochromatic beam. DFT calculations were performed by the Gaussian 03 program package at the B3LYP/6-31G basis set. The electrochemical impedance measurements were carried out in the dark state at bias potentials ranging from −0.40 to −0.65 V by using a Solartron 1287 potentiostat and a Solartron 1260 frequency-response detector. The magnitude of the sinusoidal perturbations was 10 mV, and the applied frequency range was 10^{-1}−10^5 Hz. The obtained spectra were fitted by using ZView software with the equivalent-circuit model shown in the inset of Figure 3a. The equivalent-circuit model is composed of a series resistance (R_s) and the impedance at the electrolyte/Pt counter electrode (R_{Pt} and CPE_1) and at the electrolyte/TiO_2/dye interface (R_{ct} and CPE_2).[17] The chemical capacitance (C_μ) of the TiO_2 electrode can be evaluated from CPE_2.[18]

RESULTS AND DISCUSSION

Structures and Synthesis Routes of Organic Dyes. The structures and the synthesis routes of the **M** series are shown in Chart 1 and Scheme 1, respectively. On the basis of the chemical structure of the conventional D-π-A organic dye, **M9** and **M10** were designed by incorporating thienothiophene-thiophene (for **M9**) and thienothiophene-3,4-ethylenedioxy-thiophene (for **M10**) as π-bridges. **M9** and **M10** were prepared in moderate yields using inexpensive materials and facile synthetic procedures including Suzuki coupling and Ullmann

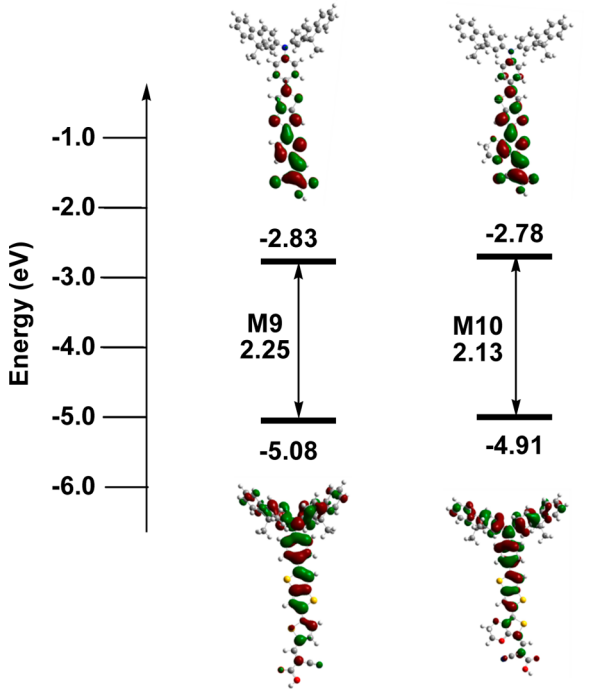

Figure 1. Calculated frontier molecular orbitals and HOMO and LUMO energy levels of the **M9** and **M10**.

dx.doi.org/10.1021/am405686z | ACS Appl. Mater. Interfaces 2014, 6, 4102−4108

Table 1. Optical and Electrochemical Data for M9 and M10

	absorption[a]				oxidation potential data		
dye	λ_{max}/nm	ε/[M^{-1} cm^{-1}]	λ_{max}/nm (on TiO_2)[b]	dye loading [10^{-7} mol cm^{-2}]	E^1_{ox}, E_{ox}[c] V vs NHE	E_{0-0}[d] eV	E^*_{ox}[e] V vs NHE
M9	436	46,269	408	5.5	1.10	2.25	−1.15
M10	469	29,067	473	4.8	1.04	2.28	−1.24

[a]Recorded in chloroform solutions at 298 K. [b]Recorded on nanocrystalline TiO_2 films. [c]Recorded in THF solution. Oxidation potentials measured versus Fc^+/Fc (E_{ox} = 0.85 V versus Ag/Ag^+) were converted to normal hydrogen electrode (NHE) by the addition of +0.63 V. [d]E_{0-0} is the optical band gap determined from the absorption onset in the UV−vis spectra. [e]E^*_{ox} was calculated by $E_{0-0} - E^1_{ox}$.

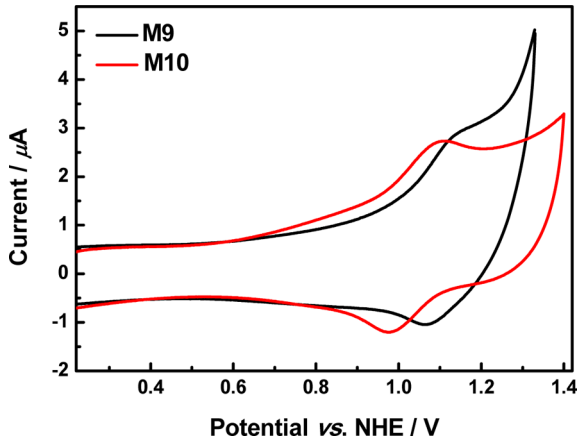

Figure 2. Cyclic voltammograms of **M9** and **M10** in THF.

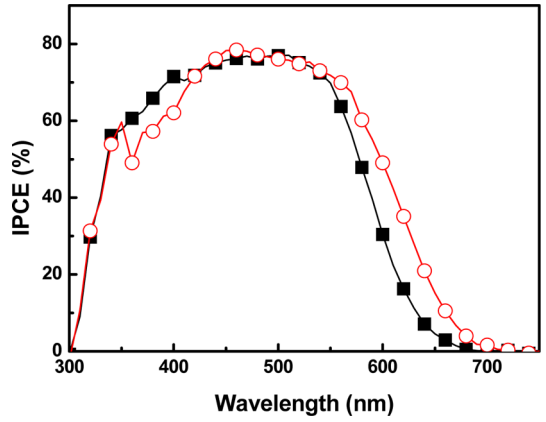

Figure 3. IPCE spectra for the DSSCs based on **M9** and **M10**.

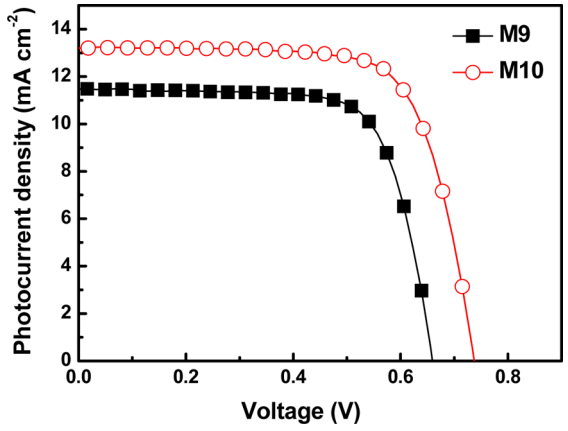

Figure 4. $J-V$ curves (light intensity: 100 mW cm^{-2}, AM 1.5 G filter) for the DSSCs based on **M9** and **M10**.

Table 2. Summary of the $J-V$ Characteristics for DSSCs Based on M9, M10, and N719[a]

dye	J_{sc}/mA cm^{-2}	V_{oc}/mV	FF/%	η/%
M9[b]	11.51 ± 0.20	669.5 ± 10.5	73.14 ± 0.60	5.67 ± 0.18
M10[b]	13.26 ± 0.21	731.8 ± 11.5	72.30 ± 0.33	7.00 ± 0.04
N719[c]	12.50 ± 0.31	804.6 ± 11.3	72.41 ± 1.63	7.24 ± 0.10

[a]Measured under irradiation of AM 1.5 G simulated solar light (100 mW cm^{-2}) at 23 °C, TiO_2 photoelectrode of 15 μm film thickness, and 0.45 cm^2 working area. [b]The concentrations of dyes are 0.5 mM in $CHCl_3$ and 0.6 M tetrabutylammonium iodide (TBAI), 0.1 M LiI, 0.05 M I_2, and 0.5 M 4-*tert*-butylpyridine (TBP) in acetonitrile as electrolyte. [c]The concentrations of dyes are 0.5 mM in EtOH and 0.05 M guanidine thiocyanate, 0.03 M I_2, 0.5 M 4-*tert*-butylpyridine (TBP), and 0.7 M 1-propyl-3-methylimidazolium (PMII) in acetonitrile mixed with valeronitrile (85/15, v/v) as electrolyte. All values were averaged from four DSSCs for each dye.

and Knoevenagel reactions. Briefly, starting material **1** was synthesized from fluorine *via* several steps,[19] and then, compound **2** was prepared from compound **1** with thieno[3,2-*b*]thiophene-2-ylboronic acid by the Suzuki reaction. Compound **3** was synthesized from compound **2** by boration using 2-isopropoxy-4,4,5,5-tetramethyl-1,3,2-dioxaborolane and, subsequently, was reacted with 5-bromo-2-thiophenecarboxaldehyde and 7-bromo-2,3-dihydrothieno[3,4-*b*][1,4]dioxine-5-carbaldehyde by means of the Suzuki reaction to yield the aldehyde derivatives **4** and **5**, respectively. From the aldehyde derivatives **4** and **5**, the final compounds **M9** and **M10** were prepared, respectively, by the Knoevenagel reaction using cyanoacetic acid with piperidine. The chemical structures of the synthesized **M** series were characterized by ^{1}H NMR, ^{13}C NMR, and mass spectroscopy.

Theoretical Calculations. DFT calculations were carried out at the B3LYP/6-31G level to obtain the HOMO and LUMO electron density surfaces for the frontier molecular orbitals (Figure 1).[20] The dihedral angles between thieno[3,2-*b*]thiophen unit and thiophene derivatives were similar, meaning that the ethylene glycol group of EDOT did not affect the conjugation along the chromophore moieties (Supporting Information Figure S1). At the HOMO level, the electron is uniformly delocalized from the donor to the π-bridge for both **M9** and **M10**, which is a suitable feature for an efficient electron transfer.[21] As a result, despite the short π-conjugation lengths, the calculated zeroth−zeroth energies (E_{0-0}) for both dyes are relatively small (2.25 and 2.33 eV for **M9** and **M10**, respectively), which can lead to a wide-range spectral absorption.

Optical and Electrochemical Properties. The UV−vis absorption spectra of the **M** series in $CHCl_3$ solution and on a nanocrystalline TiO_2 film are shown in Supporting Information Figure S2, and the obtained optical data are listed in Table 1. In $CHCl_3$ solution, the absorption peak maxima were observed at 436 and 469 nm for **M9** and **M10**, respectively. These

dx.doi.org/10.1021/am405686z | ACS Appl. Mater. Interfaces 2014, 6, 4102−4108

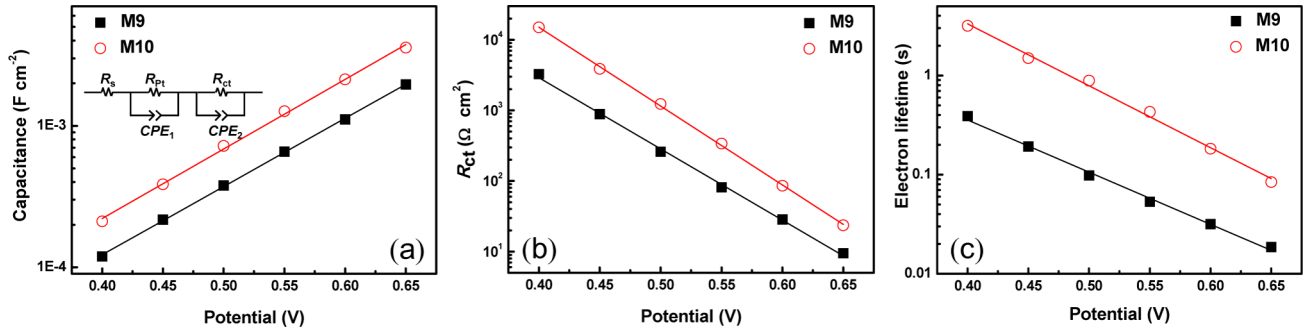

Figure 5. Chemical capacitance (a) (inset: equivalent circuit model), charge transfer resistance (b), and electron lifetime (c) for the DSSCs based on **M9** and **M10**, calculated from the impedance spectra in the dark state.

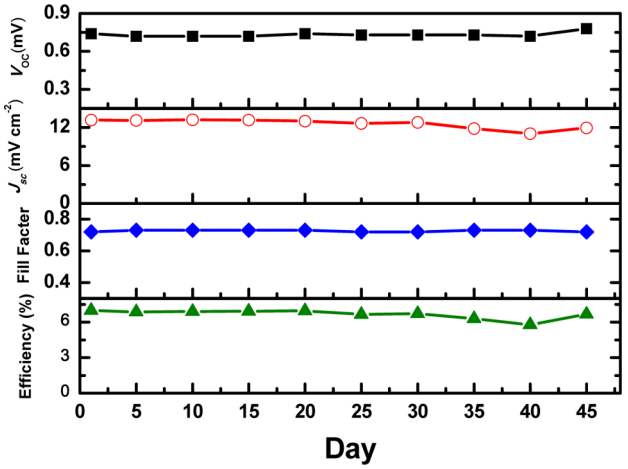

Figure 6. Long-term stability of the DSSCs based on **M10** under light soaking (light intensity: 100 mW cm^{-2}; AM 1.5 G filter).

absorption peaks may be attributed to the intramolecular charge transfer (ICT) process between the triarylamine (donor) and cyanoacrylic acid (acceptor).[22] On the 3 μm-thick nanocrystalline TiO_2 films, the absorption peak maximum was blue-shifted by 28 nm for **M9** and red-shifted by 4 nm for **M10**. It is conjectured that the blue- and red-shifts of the absorption peaks on the TiO_2 film are the consequences of *H*- and *J*-aggregation, respectively.[23] In order to compare the amount of dye loading for **M9** and **M10**, the adsorbed dye molecules on the 10 μm-thick nanocrystalline TiO_2 films were desorbed in 1 M NaOH aqueous solution and then examined by UV–vis spectroscopy. As listed in Table 1, **M10** displayed a similar amount of dye loading (5.5×10^{-7} mol cm^{-2}) compared to **M9** (4.8×10^{-7} mol cm^{-2}) in spite of the larger molecular size. The E_{0-0} values were determined from the UV–vis spectra, and the E_{ox} corresponding to the HOMO energy levels was evaluated from the cyclic voltammograms (Figure 2, Table 1). The HOMO–LUMO energy gaps, i.e., the E_{0-0} of **M9** and **M10**, were very similar to those obtained from the DFT calculations. Since both dyes have the same electron donor unit (triarylamine), the E_{HOMO} of each dye was similar, i.e., 1.10 and 1.04 V (versus NHE) for **M9** and **M10**, respectively. Compared to the redox potential of I^-/I_3^- (0.42 V versus NHE),[24] the HOMO energy levels of both dyes are sufficiently positive to be regenerated by I^- ions in the DSSC. In addition, considering the E_{cb} of TiO_2 (−0.28 V versus NHE),[25] the E_{ox}^* values, corresponding to the LUMO energy levels of both dyes, are sufficiently negative for effective electron injection into the conduction band of TiO_2.

Photovoltaic Properties. The prepared **M9** and **M10** were applied in DSSCs as photosensitizers. TiO_2 films composed of a 10 μm-thick nanoparticle layer and a 5 μm-thick scattering layer were used as photoanodes in the DSSCs. A black aperture mask was attached on the assembled devices during the measurements to prevent additional illumination through the lateral space. Figure 3 shows the IPCE as a function of the incident wavelength. Both dyes exhibited a high maximum IPCE of ~80% at 490 and 520 nm for **M9** and **M10**, respectively. The onset wavelength of IPCE spectrum was ~650 and ~675 nm for **M9** and **M10**, respectively, which coincided with the trend seen in the absorption spectra (Supporting Information Figure S2).

The *J*–*V* characteristics of the DSSCs based on **M9** and **M10** are shown in Figure 4 and summarized in Table 2. For comparison, the photovoltaic properties of the DSSC with the conventional Ru-based dye **N719** were also characterized. All values in Table 2 were averaged from four DSSCs for each dye (Supporting Information Table S1). As listed in Table 2, the conversion efficiency (η) of **M10** was higher than that of **M9** by ~27% because of the greater short-circuit photocurrent (J_{sc}) and open-circuit voltage (V_{oc}). The broader range of light absorption for **M10** compared to **M9** may contribute to the higher J_{sc}, as confirmed by the IPCE spectra. In addition, the bulky character of the 3,4-ethylenedioxythiophene (EDOT) unit in **M10** may effectively suppress the electron recombination between the TiO_2 photoanode and the electrolyte, which can contribute to the higher V_{oc} and J_{sc}. Under the same experimental conditions, **M10** exhibited a conversion efficiency (η = 7.00%) comparable to **N719** (η = 7.24%), implying that **M10** is a promising alternative to the conventional Ru-based dye.

Electrochemical Impedance Analysis. Electrochemical impedance analysis was performed to investigate the origin of the higher V_{oc} for **M10** compared to **M9**. The impedance spectra were obtained in the dark state at bias potentials ranging from −0.40 to −0.65 V. The fitted impedance parameters are plotted in Figure 5 as a function of the bias potential. As shown in Figure 5a, the TiO_2 electrode with **M10** exhibited a higher chemical capacitance (C_μ) than **M9** at the same bias potential, which may be related to the dipole moment induced by the adsorbed dye molecules.[26] In addition, as shown in Figure 5b, the TiO_2 electrode with **M10** showed higher interfacial charge transfer resistance (R_{ct}) than that with **M9** at the same bias potential, implying that the electron recombination rate between the TiO_2 electrode and the electrolyte is lower for **M10** compared to **M9**. This may be due to the blocking effect of the bulky EDOT group in **M10**,

dx.doi.org/10.1021/am405686z | ACS Appl. Mater. Interfaces 2014, 6, 4102–4108

which effectively suppresses the approach of I_3^- ions in the electrolyte to the TiO_2 surface.[27] Consequently, the electron lifetime calculated by the product of R_{ct} and C_μ was much greater for **M10** than for **M9**, as shown in Figure 5c. This difference in the electron lifetime resulted in the much higher V_{oc} of **M10** compared to **M9**.

Long-Term Stability Test. Under light soaking conditions (100 mW cm^{-2}), as shown in Figure 6, the DSSCs based on **M10** maintained nearly the initial values for all photovoltaic parameters (J_{sc}, V_{oc}, and FF) over a period of 45 days. As a result, the DSSCs based on **M10** maintained 95% of the initial conversion efficiency, respectively, after light soaking for 45 days. This remarkable long-term stability indicates that the molecular design proposed in this study is a promising method to develop reliable organic dyes for DSSCs.

CONCLUSION

In this study, we developed new D-π-A organic dyes by incorporating thieno[3,2-*b*]thiophene-thiophene (**M9**) and thieno[3,2-*b*]thiophene-EDOT (**M10**) as π-bridges. These dyes exhibited relatively small HOMO−LUMO energy gaps in spite of the short π-conjugation lengths, resulting in broad spectral responses. As photosensitizers in DSSCs, **M10** showed a much higher conversion efficiency (η = 7.00%) than **M9** (η = 5.67%) because of the broader spectral response and greater electron lifetime of the photoanode. The impedance analysis revealed that the greater electron lifetime of the photoanode with **M10** was attributed to the lower electron recombination rate resulting from the blocking effect of the bulky EDOT unit. **M10** exhibited not only a high conversion efficiency, comparable to that of the conventional Ru-based dye **N719** (η = 7.24%), but also a remarkable long-term stability; i.e., 95% of the initial conversion efficiency was maintained after light soaking for 45 days (1080 h). These results imply that the molecular design proposed in this study is a promising approach to developing organic dyes that satisfy the requirements of high efficiency and stability.

ASSOCIATED CONTENT

Supporting Information

Theoretical calculations for dihedral angles, UV−vis absorption spectra, and *J*−*V* characteristics. This information is available free of charge via the Internet at http://pubs.acs.org.

AUTHOR INFORMATION

Corresponding Authors

*E-mail: mjko@kist.re.kr.

*E-mail: dhlee@sogang.ac.kr.

Notes

The authors declare no competing financial interest.

ACKNOWLEDGMENTS

This work was supported by the National Research Foundation of Korea (NRF) grants funded by the Ministry of Science, ICT & Future Planning (MSIP) of Korea under contract Nos. 2012M3A6A7054856 (the Global Frontier R&D Program on Center for Multiscale Energy System) and 2012-0005955 (the Pioneer Research Program) and 2013 University-Institute cooperation program. This work was also funded by the KIST institutional programs (2V03230 and 2E24821).

REFERENCES

(1) O'Regan, B.; Grätzel, M. A Low-Cost, High-Efficiency Solar Cell Based on Dye-Sensitized Colloidal TiO_2 Films. *Nature* **1991**, *353*, 737−740.

(2) Nazeeruddin, M. K.; Angelis, F. D.; Fantacci, S.; Selloni, A.; Viscardi, G.; Liska, P.; Ito, S.; Takeru, B.; Grätzel, M. Combined Experimental and DFT-TDDFT Computational Study of Photoelectrochemical Cell Ruthenium Sensitizers. *J. Am. Chem. Soc.* **2005**, *127* (48), 16835−16847.

(3) Yasuo, C.; Ashraful, I.; Yuki, W.; Ryoichi, K.; Naoki, K.; Liyuan, H. Dye-Sensitized Solar Cells with Conversion Efficiency of 11.1%. *Jpn. J. Appl. Phys., Part 2* **2006**, *45*, L638−L640.

(4) Numata, Y.; Islam, A.; Chen, H.; Han, L. Aggregation-Free Branch-Type Organic Dye with a Twisted Molecular Architecture for Dye-Sensitized Solar Cells. *Energy Environ. Sci.* **2012**, *5*, 8548−8552.

(5) Hagfeldt, A.; Grätzel, M. Molecular Photovoltaics. *Acc. Chem. Res.* **2000**, *33* (5), 269−277.

(6) Pei, K.; We, Y.; Islam, A.; Zhang, Q.; Han, L.; Tian, H.; Zhu, W. Constructing High-Efficiency D-A-π-A-Featured Solar Cell Sensitizers: A Promising Building Block of 2,3-Diphenylquinoxaline for Antiaggregation and Photostability. *ACS Appl. Mater. Interfaces* **2013**, *5*, 4986−4995.

(7) Ying, W.; Yang, J.; Wielopolski, M.; Moehl, T.; Moser, J.; Comte, P.; Hua, J.; Zakeeruddin, S.; Tian, H.; Grätzel, M. New Pyrido[3,4-*b*]pyrazine-Based Sensitizers for Efficient and Stable Dye-Sensitized Solar Cells. *Chem. Sci.* **2014**, *5*, 206−214.

(8) Cai, S.; Hu, X.; Zhang, Z.; Su, J.; Li, X.; Islam, A.; Han, L.; Tian, H. Rigid Triarylamine-Based Efficient DSSC Sensitizers with High Molar Extinction Coefficients. *J. Mater. Chem. A* **2013**, *1*, 4763−4772.

(9) Cai, S.; Tian, G.; Li, X.; Su, J.; Tian, H. Efficient and Stable DSSC Sensitizers Based on Substituted Dihydroindolo[2,3-*b*]carbazole Donors with High Molar Extinction Coefficients. *J. Mater. Chem. A* **2013**, *1*, 11295−11305.

(10) Zhu, W.; Wu, Y.; Wang, S.; Li, W.; Li, X.; Chen, J.; Wang, Z.-S.; Tian, H. Organic D-A-π-A Solar Cell Sensitizers with Improved Stability and Spectral Response. *Adv. Funct. Mater.* **2011**, *21* (4), 756−763.

(11) Kim, S.; Choi, H.; Kim, D.; Song, K.; Kang, S. O.; Ko, J. Novel Conjugated Organic Dyes Containing Bis-dimethylfluorenylamino phenyl Thiophene for Efficient Solar Cell. *Tetrahedron* **2007**, *63*, 9206−9212.

(12) Jung, I.; Lee, J. K.; Song, K. H.; Song, K.; Kang, S. O.; Ko, J. Synthesis and Photovoltaic Properties of Efficient Organic Dyes Containing the Benzo[*b*]furan Moiety for Solar Cells. *J. Org. Chem.* **2007**, *72*, 3652−3658.

(13) Wang, Z.-S.; Koumura, N.; Cui, Y.; Takahashi, M.; Sekiguchi, H.; Mori, A.; Kubo, T.; Furube, A.; Hara, K. Hexylthiophene-Functionalized Carbazole Dyes for Efficient Molecular Photovoltaics: Tuning of Solar-Cell Performance by Structural Modification. *Chem. Mater.* **2008**, *20*, 3993−4003.

(14) Choi, H.; Raabe, I.; Kim, D.; Teocoli, F.; Kim, C.; Song, K.; Yum, J.-H.; Ko, J.; Nazeeruddin, M. K.; Grätzel, M. High Molar Extinction Coefficient Organic Sensitizers for Efficient Dye-Sensitized Solar Cells. *Chem.−Eur. J.* **2010**, *16*, 1193−1201.

(15) Koo, H.-J.; Park, J.; Yoo, B.; Yoo, K.; Kim, K.; Park, N.-G. Size-Dependent Scattering Efficiency in Dye-Sensitized Solar Cell. *Inorg. Chim. Acta* **2008**, *361*, 677−683.

(16) Fabregat-Santiago, F.; Bisquert, J.; Garcia-Belmonte, G.; Boschloo, G.; Hagfeldt, A. Influence of Electrolyte in Transport and Recombination in Dye-Sensitized Solar Cells Studied by Impedance Spectroscopy. *Sol. Energy Mater. Sol. Cells* **2005**, *87*, 117−131.

(17) Kim, J.-Y.; Kim, J. Y.; Lee, D.-K.; Kim, B.; Kim, H.; Ko, M. J. Importance of 4-tert-Butylpyridine in Electrolyte for Dye-Sensitized Solar Cells Employing SnO_2 Electrode. *J. Phys. Chem. C* **2012**, *116*, 22759−22766.

(18) Park, J.; Koo, H.-J.; Yoo, B.; Kim, K.; Choi, W.; Park, N.-G. On the *I*−*V* Measurement of Dye-Sensitized Solar Cell: Effect of Cell Geometry on Photovoltaic Parameters. *Sol. Energy Mater. Sol. Cells* **2007**, *91*, 1749−1754.

(19) Shirota, Y.; Kinoshita, M.; Noda, T.; Okumoto, K.; Ohara, T. A Novel Class of Emitting Amorphous Molecular Materials as Bipolar Radical Formants: 2-{4-[Bis(4-methylphenyl)amino]phenyl}-5-(dimesitylboryl)thiophene and 2-{4-[Bis(9,9-dimethylfluorenyl)-amino]phenyl}-5-(dimesitylboryl)thiophene. *J. Am. Chem. Soc.* **2000**, *122* (44), 11021−11022.
(20) Stephens, P. J.; Devlin, F. J.; Chablowski, C. F.; Frisch, M. Ab Initio Calculation of Vibrational Absorption and Circular Dichroism Spectra Using Density Functional Force Fields. *J. Phys. Chem.* **1994**, *98*, 11623−11627.
(21) Cai, L.; Tsao, H. N.; Zhang, W.; Wang, L.; Xue, Z.; Grätzel, M.; Liu, B. Organic Sensitizers with Bridged Triphenylamine Donor Units for Efficient Dye-Sensitized Solar Cells. *Adv. Energy Mater.* **2013**, *3* (2), 200−205.
(22) Roquet, S.; Cravino, A.; Leriche, P.; Alévêque, O.; Frère, P.; Roncali, J. Triphenylamine-Thienylenevinylene Hybrid Systems with Internal Charge Transfer as Donor Materials for Heterojunction Solar Cells. *J. Am. Chem. Soc.* **2006**, *128* (10), 3459−3466.
(23) Verma, S.; Ghosh, H. N. Exciton Energy and Charge Transfer in Porphyrin Aggregate/Semiconductor (TiO_2) Composites. *J. Phys. Chem. Lett.* **2012**, *3*, 1877−1884.
(24) Clifford, J. N.; Palomares, E.; Nazeeruddin, M. K.; Grätzel, M.; Durrant, J. R. Dye Dependent Regeneration Dynamics in Dye Sensitized Nanocrystalline Solar Cells: Evidence for the Formation of a Ruthenium Bipyridyl Cation/Iodide Intermediate. *J. Phys. Chem. C* **2007**, *111*, 6561−6567.
(25) Grätzel, M. Photoelectrochemical Cells. *Nature* **2001**, *414*, 338−344.
(26) Chen, P.; Yum, J. H.; Angelis, F. D.; Mosconi, E.; Fantacci, S.; Moon, S.-J.; Baker, R. H.; Ko, J.; Nazeeruddin, M. K.; Grätzel, M. High Open-Circuit Voltage Solid-State Dye-Sensitized Solar Cells with Organic Dye. *Nano Lett.* **2009**, *9* (6), 2487−2492.
(27) Liu, W.-H.; Wu, I.-C.; Lai, C.-H.; Lai, C.-H.; Chou, P.-T.; Li, Y.-T.; Chen, C.-L.; Hsu, Y.-Y.; Chi, Y. Simple Organic Molecules Bearing a 3,4-Ethylenedioxythiophene Linker for Efficient Dye-Sensitized Solar Cells. *Chem. Commun.* **2008**, 5152−5154.